ISSN 1063-7842, Technical Physics, 2017, Vol. 62, No. 7, pp. 1006–1012. © Pleiades Publishing, Ltd., 2017.
Original Russian Text © N.N. Simakov, 2017, published in Zhurnal Tekhnicheskoi Fiziki, 2017, Vol. 87, No. 7, pp. 990–996.

GASES AND LIQUIDS

Numerical Simulation of the Two-Phase Flow Produced by Spraying a Liquid by a Nozzle

N. N. Simakov

Yaroslavl State Technical University, Yaroslavl, 150023 Russia
e-mail: nik_simakov@mail.ru

Received October 12, 2016

Abstract—A numerical experiment on the simulation of the two-phase flow formed during spraying of a liquid by a nozzle has been described. The radial and axial velocity profiles of the droplets and gas in the free spray and in the two-phase flow through a cylindrical apparatus have been calculated and represented taking into account the early drag crisis of droplets and peculiarities of turbulent friction in the gas, which was detected in previous experiments. The distinguishing feature of the numerical model of the two-phase flow is that it employs the differential equations describing the nonstationary flow of a compressible gas as the initial equations. In transition to their difference analog, the familiar Lax–Wendorff algorithm has been used. A comparison of the results of calculations based on this model with experimental data has demonstrated their concordance.

DOI: 10.1134/S1063784217070222

INTRODUCTION: PECULIARITIES OF THE TWO-PHASE FLOW IN THE SPRAY

Spraying of a liquid in a gas, e.g., using atomizers, is often used to intensify a number of technological heat- and mass-transfer processes, such as the combustion of liquid fuels, drying, graining of polymers, and cleaning of air from dust and gas impurities. In analyzing these processes, it is important to know the hydrodynamic structure of the two-phase flow being formed, which is known as the spray, and the forces of interaction between droplets and the gas. Satisfactory methods for designing spraying processes have not yet been developed, which makes this study topical.

The simulation of the spray can be carried out using one of two approaches, i.e., the interpenetrating continuums method [1] or the turbulent jet theory [2]. In the former approach, both phases are considered to be distributed continuously over the space with the variable density averaged over a small volume and with different velocities. In the latter approach, it is assumed that the concentration of the dispersed phase is relatively low, and the velocities of the phases are approximately identical; however, the turbulence of the gas-phase flow is taken into account. Each of these approaches considered separately disregards some important features of the spray hydrodynamics, including the following factors.

It has been established experimentally that the gas flow in the spray is a turbulent jet [3, 4]. This jet is formed at the root of the spray due to the interaction between phases and subsequently evolves as if autonomously from the droplet flow. This jet differs from the one-phase flow in the structure and the type of turbulent friction. In particular, dimensionless profiles of the axial velocity of the gas turn out to be slightly different (more gently sloping) than in a one-phase jet. It has been established that the velocities of the phases at each point of the flow are different, and the gas pressure differences on the order of 1–10 Pa exist along the spray axis and radius.

In addition, the substantial peculiarity in the interaction between the phases (early drag crisis) has been detected. This should be taken into account in calculating the spray and can be explained as follows.

In processes involving the spraying of a liquid, droplets with average diameter d on the order of 10^{-4} m are formed. With this size and a large difference in the dynamic viscosities of the liquid in droplets and of the gas flowing past them (by about 60 times in the case of water and air), the deformation of droplets and the internal flow of the liquid in them can be disregarded, treating droplets as hard spheres.

The hydrodynamic drag force acting a droplet in a gas flow can be calculated as

$$F = C_d S \rho V^2/2, \quad (1)$$

which requires the knowledge of the relative velocity V of a droplet in the gas and the hydrodynamic drag coefficient C_d. Here and below, $S = \pi d^2/4$ is the midsection area of a spherical droplet, ρ is the gas density, and μ is the dynamic viscosity of the gas.

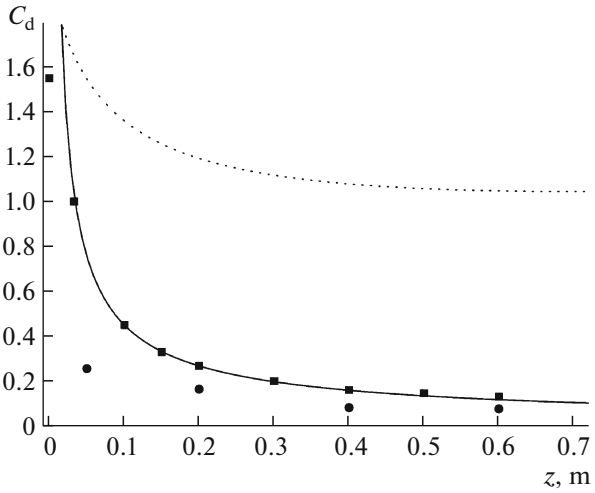

Fig. 1. Dependence of drag coefficient C_d of droplets at distance z from the nozzle: (■) experimental results [3] with water droplets on the spray axis under water pressure $P_l = 5 \times 10^5$ Pa at the sprayer; (●) same at points of the spray boundaries; solid curve is an approximation of experimental results on spray axis by formula (15); dashed curve is calculated by formula (3) using experimental data from [3] for velocities of gas and droplets and their sizes.

For a sphere in a laminar flow with small Reynolds numbers $\mathrm{Re} = Vd\rho/\mu \ll 1$, the Stokes formula is valid as follows:

$$C_d = 24/\mathrm{Re}, \tag{2}$$

while for a sphere and the transient range $2 < \mathrm{Re} < 700$, the Klyachko dependence holds, i.e.,

$$C_d = 24/\mathrm{Re} + 4/\mathrm{Re}^{1/3}, \tag{3}$$

which successfully approximates the experimental data generalized by the Rayleigh curve in the given range [5, 6].

It was shown in [3, 4] using experimental data (Fig. 1) that the value of C_d for droplets in a strongly turbulent flow with $\mathrm{Re} \approx 100$ is smaller by a factor of four to seven compared to the well-known values determined by formula (3). An analogous early drag crisis was also observed for a solitary hard sphere in a gas jet flowing through a confuser [7]. It should be noted that experimental points shown in Fig. 1 for $z > 0.15$ m are close to the values that correspond to Stokes formula (2).

As a reason explaining the early drag crisis for a spherical particle, the hypothesis was put forth in [7] concerning the effect of strong turbulence of the gas flow, which could be intensified by the confuser still further (as compared to a free jet) so that it became sufficient for the emergence of an early crisis at a solitary hard sphere. This hypothesis was confirmed by a numerical experiment on a sphere in a free gas flow (both laminar and strongly turbulent) [8]. The above arguments lead to the conclusion that it is expedient to use a combination of the two above-mentioned approaches (method of interpenetrating continuums [1] and the theory of turbulent jets [2]) in mathematical and numerical simulation of a spray as a two-phase flow, taking into account all its peculiarities to describe the motion of both phases in a unified manner. An analogous idea was used earlier in [4, 9], but to a limited extent (on a domain of calculation with a smaller number of points, 26×26, and only for a free spray unbounded by the apparatus walls).

1. MATHEMATICAL MODEL OF A FREE SPRAY

A turbulent flow of the gas phase in the cylindrical system of coordinate can be described by the time-dependent continuity equation

$$\frac{\partial \rho}{\partial t} + \frac{\partial(\rho w_z)}{\partial z} + \frac{1}{\rho}\frac{\partial(r\rho w_r)}{dr} = 0 \tag{4}$$

and the equation of motion for the time-averaged axial ($w_z = w_z(r, z)$) and radial ($w_r = w_r(r, z)$) gas velocity components as follows:

$$\frac{\partial w_z}{\partial t} + w_z\frac{\partial w_z}{\partial z} + w_r\frac{\partial w_z}{\partial r} = \frac{1}{\rho r}\frac{\partial(r\tau)}{\partial r} - \frac{1}{\rho}\frac{\partial P}{\partial z} + \frac{f_z}{\rho}, \tag{5}$$

$$\frac{\partial w_r}{dt} + w_z\frac{\partial w_r}{\partial z} + w_r\frac{\partial w_r}{\partial r} = -\frac{1}{\rho}\frac{\partial P}{\partial r} + \frac{f_r}{\rho}. \tag{6}$$

Analogous equations are used for the liquid phase (subscript "l"):

$$\frac{\partial \alpha}{\partial t} + \frac{\partial(\alpha u_z)}{\partial z} + \frac{1}{r}\frac{\partial(r\alpha u_r)}{dr} = 0, \tag{7}$$

$$\frac{\partial u_z}{\partial t} + u_z\frac{\partial u_z}{\partial z} + u_r\frac{\partial u_z}{\partial r} = -\frac{f_z}{\alpha\rho_l}, \tag{8}$$

$$\frac{\partial u_r}{\partial t} + u_z\frac{\partial u_r}{\partial z} + u_r\frac{\partial u_r}{\partial r} = -\frac{f_r}{\alpha\rho_l}. \tag{9}$$

Here, ρ and P are the gas density and pressure, τ is the turbulent drag stress in the gas phase, f_r and f_z are the volume densities of the interfacial interaction forces, α is the relative volume of the liquid (porosity), ρ_l is the physical density of droplets, and u_z and u_r are the axial and radial velocity components of the liquid.

System of equations (4)–(9) is not closed since it contains nine unknown functions, i.e., w_z, w_r, ρ, P, α, u_z, u_r, f_r, and f_z. The closure of the system can be performed as follows.

First, we can assume that the gas flow in the spray is adiabatic and use the equation of the Poisson adiabat:

$$\frac{P}{\rho^\gamma} = \mathrm{const} = \frac{P_0}{\rho_0^\gamma}, \tag{10}$$

which leads to the relations

$$dP = \gamma \frac{P}{\rho} d\rho = c^2 d\rho = c_0^2 \left(\frac{\rho}{\rho_0}\right)^{\gamma-1} d\rho, \quad (11)$$

where c is the velocity of sound in the gas, γ is the adiabatic exponent, and subscript "0" marks the initial values of the quantities.

Substituting the last term from (11) into expressions (5) and (6), we can eliminate gas pressure P from system of equations (4)–(9).

Second, based on experimental data, the following expression was obtained in [4] for gas turbulent drag stress τ:

$$\tau = -\rho \frac{rZ}{2\zeta^2} \left(\frac{\partial w_r}{\partial r}\right)^2, \quad (12)$$

where $Z = z + Z_0$ is the axial coordinate measured from the gas jet pole, z is the same measured from the sprayer, Z_0 is the distance from the pole to the sprayer, and $\zeta = \text{const}(P_l)^{1/2}$. For excess water pressure $P_l = 5 \times 10^5$ Pa at the sprayer, values of $Z_0 = 390$ mm and $\zeta = 11.9$ were obtained.

It should be noted that representation (12) differs from an analogous representation for a one-phase turbulent gas jet in accordance with the new Prandtl hypothesis as follows:

$$\tau = \rho l^2 \left(\frac{\partial w_z}{\partial r}\right)^2 = \rho \nu_t \frac{\partial w_z}{\partial r}, \quad (13)$$

where l is the mixing length. For a circular jet, the kinematic turbulent viscosity $\nu_t = \text{const}$ is an empirical constant [10]. It should be noted that, by substituting expression (12) into Eq. (5), we can disregard the dependence of ρ on r in the subsonic flow for simplifying the latter equation.

Third, the drag exerted by the gas on an individual droplet, which is usually expressed by formula (1), where $\mathbf{V} = \mathbf{U} - \mathbf{W}$ is the relative velocity of the droplet in the gas. Then we can write the following expression for the components of the volume density of interfacial interaction forces:

$$f_{z,r} = F_{z,r} n = \frac{F_{z,r} \alpha \rho_l}{m_d}, \quad (14)$$

where n is the number density of droplets and m_d is the mass of an individual droplet.

As noted above, the values of drag coefficient C_d for droplets in the spray and its dependence on Reynolds number $\text{Re} = \rho dV/\mu$ are anomalous [3, 4]. At the spray root near the sprayer, the values of C_d approximately correspond to the dependences well known from the literature (e.g., Klyachko formula (3)) and sharply decrease (by four to seven times) with increasing distance from the sprayer (see Fig. 1).

It can be seen from Fig. 1 that the decrease in C_d with increasing distance z from the sprayer along the spray axis is successfully approximated by the dependence

$$C_d(0, z) = 0.45(z/0.1)^{-3/4}. \quad (15)$$

At the spray boundary $r = r_{lim}(z) = z\tan\varphi$, which is determined by the remotest (from the axis) trajectories of droplets forming angle $\varphi = 32.5°$, which is half the root angle of the spray, the values of $C_d(r_{lim}, z)$ are obviously half (smaller by 1.8 times than) the value of $C_d(0, z)$ on the spray axis; this will be taken into account in further calculations in the expression

$$C_d(r, z) = C_d(0, z)(0.45\exp(-6r/r_{lim}(z)) + 0.55). \quad (16)$$

In numerical simulation of the spray, before representing the differential equations by their difference analogs, it is expedient to pass to dimensionless variables, dividing the values of coordinates r and z by the initial (minimal) radius r_0 of the spray in the computation domain; velocities w, u, V, and c_0 by initial velocity u_0 of droplets (liquid jets); and ρ by density ρ_0 by the stationary gas away from the spray, and t by $t_0 = r_0/u_0$. In this case, the form of Eqs. (4)–(9) does not change, and the terms on the right-hand sides of the equations acquire corresponding additional coefficients.

Passing from differential equations (4)–(9) to their difference analogs using representations (1), (11)–(16) on the rectangular spatial grid (i, j), as in [4, 9], we used the explicit two-step Lax–Wendorff difference scheme [11]. In this scheme, intermediate values of dependent variables are determined for each temporal layer at the first (auxiliary) step of calculation for $t = (n + 1/2)\Delta t$ using the Lax scheme with half-step $\Delta t/2$. The values of quantities on the previous layer are averaged over four nearest nodes. At the second (main) step of calculations with total time step Δt, the resultant intermediate values of quantities are used in the expressions approximating spatial derivatives, and new values of variables are determined. Then, the cycle is repeated.

The Lax–Wendorff scheme is found to be centered in time [11]; for this reason, numerical effects of viscosity and diffusion in it are much weaker then in the one-step Lax scheme, which makes it possible to obtain the velocity profiles for each phase, which are closer to their true counterparts. To ensure the stability of the difference scheme, it is necessary to satisfy the Courant–Friedrichs–Lewy conditions [11], which has the following form for identical spatial steps $\Delta z = \Delta r$ of the grid:

$$\Delta t \le \frac{\Delta z}{\sqrt{2(c^2 + w_z^2 + w_r^2)}}. \quad (17)$$

The proposed model is advantageous because its difference equations make it possible to calculate variables using a simple explicit scheme. One of difficulties encountered in constructing the numerical model is the specification of appropriate boundary condi-

tions that preserve the stability of the difference scheme. At the boundary nodes of the domain of calculation, the difference scheme inevitably has a form that differs from that at the inner points; in this scheme, spatial derivatives can be approximated using one-sided, rather than two-sided differences. In addition, one should bear in mind that radial velocities $w_r = u_r = 0$ of the phases on the symmetry axis (for $r = i\Delta r = 0$); the derivatives of some variables with respect to r can also vanish at these points.

At the upper (inlet) boundary of the domain of calculations ($j = 0$), it is necessary (taking into account experimental data) to specify the porosity profile, say, of triangular form $\alpha(r, z_0) = 3(r_n/r_0)^2(1 - r/r_0)$, r_n being the radius of the outlet apertures of the sprayer.

At the upper boundary, the radial profiles of liquid velocity components $u_z(r, z_0)$ and $u_r(r, z_0)$ are also specified. The former profile can be rectangular, trapezoidal, or more complicated, but it is expedient to specify the latter profile by the linear function of radius, $u_r(r, z_0) = u_z(r, z_0)r/z_0$ on account of the form of the liquid flow from the sprayer nozzle. Instead of the experimental data, we can use the results of previous calculations for the region closest to the sprayer.

In calculating the free spray on the lateral (external) boundary, the gas density can be determined using the Bernoulli equation

$$\rho = \rho_0\left(1 - \frac{w_z^2 + w_r^2}{2c_0^2}\right). \quad (18)$$

To calculate the two-phase flow in the spray apparatus, the conditions of vanishing of the gas velocity components ($w_z = w_r = 0$) are specified at the lateral boundary (wall of the cylindrical apparatus).

2. RESULTS OF CALCULATING THE FREE SPRAY

The above-described algorithm was realized using the Delphi program package to calculate the two-phase flow in an axisymmetric spray produced by centrifugal-spray injector with a nozzle diameter of 2 mm. During code debugging, the difference form of the boundary condition was varied, while in the numerical experiment, we varied the form of dependences (12), (13) for turbulent drag stress of the gas and the droplet drag coefficient using formulas (2), (3), and (16), as well as $C_d = 0.17$ and 0.1.

The unit of dimensionless spatial scale of the grid was the spray radius at the upper boundary $r_0 = z_0 \tan\varphi$ of the domain of calculations ($\varphi = 32.5°$ is half the root angle of the spray); for the unit of the velocity scale, the initial velocity $u_0 = 0.75(2P_l/\rho_l)^{1/2}$ of liquid flow from the sprayer nozzle was used. The calculations were performed for water pressure $P_l = 5 \times 10^5$ Pa at the sprayer; the measured droplet diameter was $d =$ 0.14 mm. In our calculations, the value of $z_0 = 100$ mm was used.

The dimensionless grid pitch was defined as $h = \Delta r = \Delta z = 1/N$, $N = 16$; the size of the spatial region was $r_{max} = \max(i)h$, $z_{max} - z_0 = \max(j)h$. The size of the rectangular grid was varied to $\max(i) = \max(j) = 200$ and ensured sufficient approximation of the difference scheme.

It has been established that the (quasi-)stationary state of the flow we are interested in the present problem was attained as a result of evolution of the time-dependent solution over the grid time, which is approximately 15–20 times longer than the characteristic time $t_s = (z_{max} - z_0)/u_0$, over which the droplets crossed the domain of calculations from the upper to lower boundary disregarding their deceleration in the gas.

Figures 2–4 show the results of calculations of a free axisymmetric spray based on the proposed model. Figure 2 shows the results of the calculation and experimental data [3] for the velocities of phases at the spray axis for the values of C_d calculated using formulas (16) and (3). In the former case, the agreement between the calculation and experiment is obvious. In the latter case, droplets are decelerated, and the gas is accelerated more intensely than in the experiment. Figure 3 shows the axial velocity profiles for the gas in the spray at distances $z = 100$, 150, 300, and 500 mm from the nozzle. Symbols show experimental results from [3], and the curves are obtained as a result of calculations. Figure 4 shows analogous profiles for droplets at distances $z = 100$, 300, and 700 mm from the sprayer. The curve for $j = 0$ and $z = 100$ mm describes the dependence that approximates the experimental data [3]. Figures 2–4 demonstrate satisfactory agreement between the results of calculations of a free spray taking into account droplet drag crisis and experiments for a considerable length of the spray region of 100–700 mm from the nozzle.

3. CALCULATION OF THE TWO-PHASE FLOW IN A SPRAYING APPARATUS

Among the spraying systems used in chemical technologies, two types can be distinguished, i.e., injectors and ejectors [12]. Both of these contain cylindrical chambers for phase mixing that is coaxial with the sprayer and a separator tank for their separation. The difference between these systems is that the gas flow rate in the injector is limited by the valve at the apparatus outlet, while the valve in the ejector is installed at the inlet.

The presence of the cylindrical chamber limits the two-phase flow in radius and height. The inner surface of its wall is the lateral boundary $i = n$ in the computation domain, on which both gas velocity components vanish: $wz(i, j) = uz(i, j) = 0$. Droplets freely precipitate on the wall. The height of the mixing chamber H

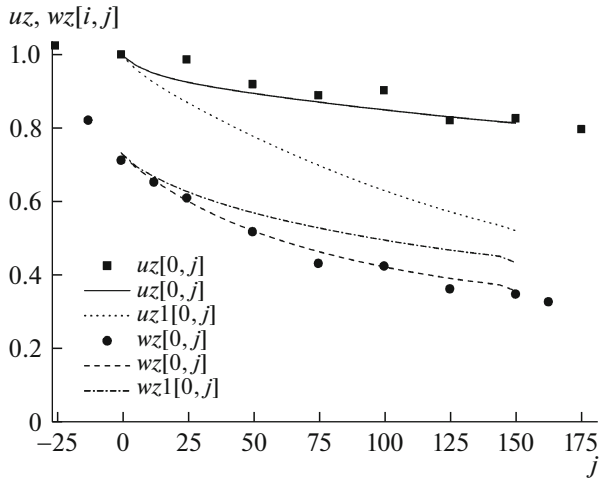

Fig. 2. Variations in velocities of droplets (uz) and gas (wz) on spray axis; curves are calculated taking into account drag crisis by formula (16); $uz1$ and $wz1$ curves are calculated using formula (3); $j = -25$ is position of the outlet aperture of the nozzle.

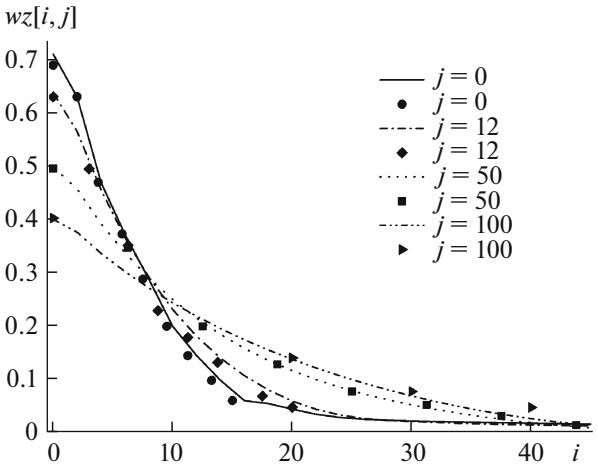

Fig. 3. Radial profiles of the axial velocity of the gas at different distances $z = (100 + 4j)$ mm from the nozzle; curves are calculation results, symbols represent experimental data.

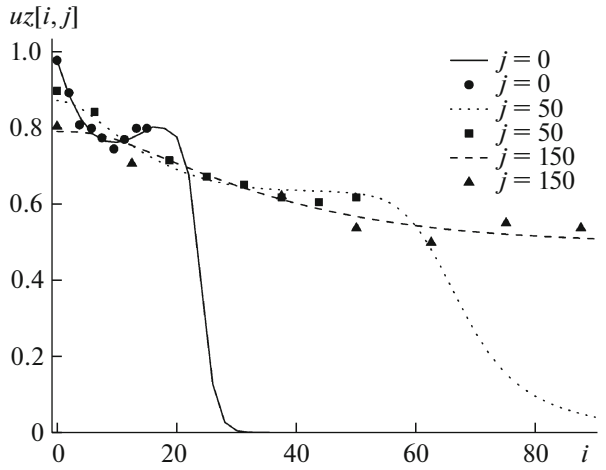

Fig. 4. Radial profiles of axial velocity of droplets at different distances $z = (100 + 4j)$ mm from the nozzle; curves are calculation results, symbols represent experimental data.

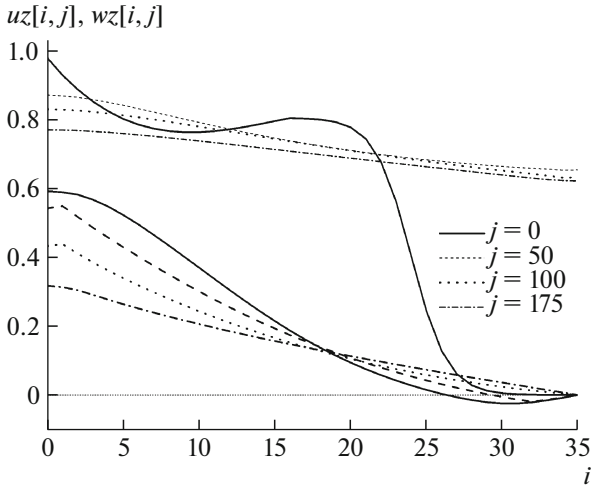

Fig. 5. Calculated axial velocity profiles for droplets (top) and gas (bottom) at different distances $z = (100 + 4j)$ mm from nozzle in spraying apparatus of diameter D_{APP} = 140 mm and height $H = 800$ mm.

is connected with the position of the lower boundary $j = nz$ of the computation domain by the relation $H = (100 + 4nz)$ mm.

In calculations, the gas pressure drop P between the lower and upper cross sections of the mixing chamber (computation domain boundaries) was specified. The volume gas flow rate Q in the apparatus was determined from the calculated values of the gas axial velocity. The variants of designing of the apparatus differed in the gas pressure drop P and diameter D_{APP} of the mixing chamber of the apparatus.

The results of calculations were used to determine the $P(Q)$ dependence known as the hydraulic characteristic of the apparatus, maximal values P_m and Q_m, their dependence on D_{APP}, as well as the dependence

$$\text{eff}(Q) = PQ/(P_l Q_l) \quad (19)$$

of the hydraulic efficiency of the apparatus on gas flow rate (P_l and Q_l are the pressure drop and the flow rate of the liquid at the sprayer. In calculations, the following experimental data for these quantities were used: $P_l = 5 \times 10^5$ Pa and $Q_l = 0.745 \times 10^{-4}$ m^3). These results are represented in Figs. 5–9.

Figure 5 shows the axial velocity profiles for droplets and gas in the apparatus for various distances z from the nozzle; Fig. 6 shows the profiles of the radial

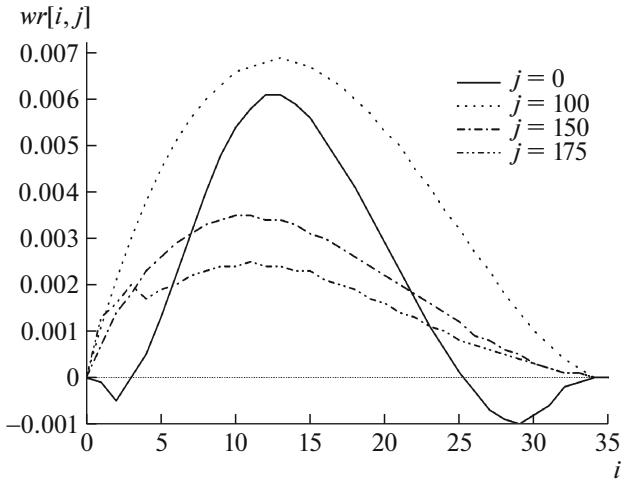

Fig. 6. Calculated radial velocity profile for the gas at distances $z = (100 + 4j)$ mm from the nozzle in the apparatus of diameter $D_{APP} = 140$ mm and height $H = 800$ mm.

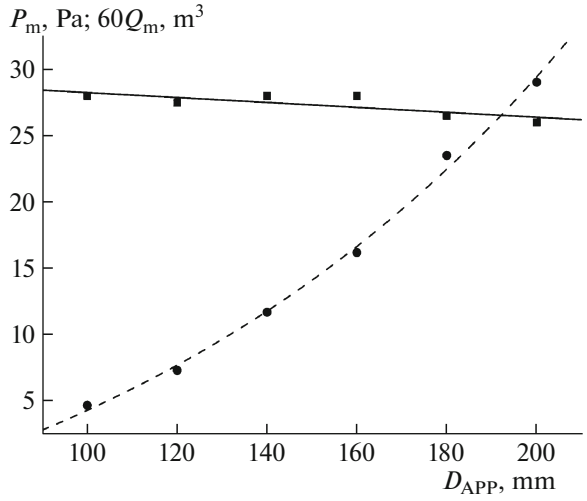

Fig. 7. Calculated dependences of maximal values of (■) pressure drop P_m of the gas in the apparatus and (●) volume flow rate Q_m of gas on apparatus diameter D_{APP}.

gas velocity in different radial cross sections of the same apparatus for the same gas pressure drop in it ($P = 14$ Pa). The negative values of the wz and wr projections of the gas velocity onto the coordinate axes near the apparatus wall ($i = 35$) indicate the reverse vortex flow of the gas near the upper ($j = 0$) inlet cross section of the apparatus.

Figure 7 shows the calculated dependences of the maximal values of the pressure drop P_m in the apparatus and volume gas flow rate Q_m on the apparatus diameter D_{APP}. It can be seen that, upon an appreciable increase in the apparatus cross-sectional area (by four times), the maximal gas pressure drop P_m across it changes insignificantly (by 7%). At the same time, the maximal gas flow rate Q_m in the apparatus changes significantly (by six times), approximately following the power law $Q_m = 0.08(10D_{APP})^{2.6}$ if Q_m is measured in cubic meters and D_{APP} in meters.

Figure 8 shows the calculated dependences of the relative pressure drop $p = P/P_m$ of the gas in the apparatus on the relative volume flow rate $q = Q/Q_m$ of the gas through the apparatus. Figure 9 shows the calculated dependences of the relative hydraulic efficiency $e = \text{eff}/\text{eff}_m$ of the apparatus on the relative volume flow rate q of the gas through the apparatus. For reference, it should be noted that $\text{eff}_m = 0.055$ for $D_{APP} = 140$ mm and $\text{eff}_m = 0.083$ for $D_{APP} = 160$ mm.

It is interesting to note that the $p(q)$ and $e(q)$ dependences obtained in [12] from simple theoretical premises, which have the simple form

$$p = 1 - q^2, \tag{20}$$

$$e = 3^{3/2}/2q(1 - q^2) \tag{21}$$

and coincide with the experimental results obtained on spraying apparatuses, were also found to be in conformity with the results of calculations based on a more rigorous model of the spray described above. This is obvious from Figs. 8 and 9.

Formula (21) implies that the maximal hydraulic efficiency eff_m of the sprayer is attained for optimal gas flow rate Q_{opt}, which satisfies the condition

$$q_{opt} = Q_{opt}/Q_m = 3^{-1/2}. \tag{22}$$

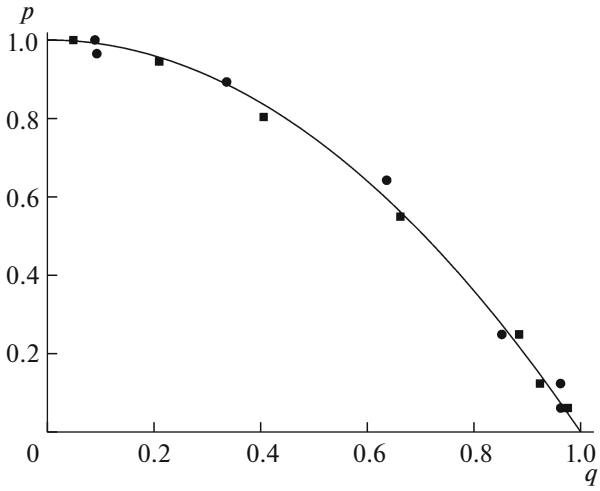

Fig. 8. Calculated dependences of relative pressure drop $p = P/P_m$ of gas in apparatus on relative volume flow rate $q = Q/Q_m$ of gas through apparatus for both diameters D_{APP}: (■) 140 and (●) 160 mm; P_m and Q_m are the maximal values of P and Q. Curve is calculated dependence $p = 1 - q^2$.

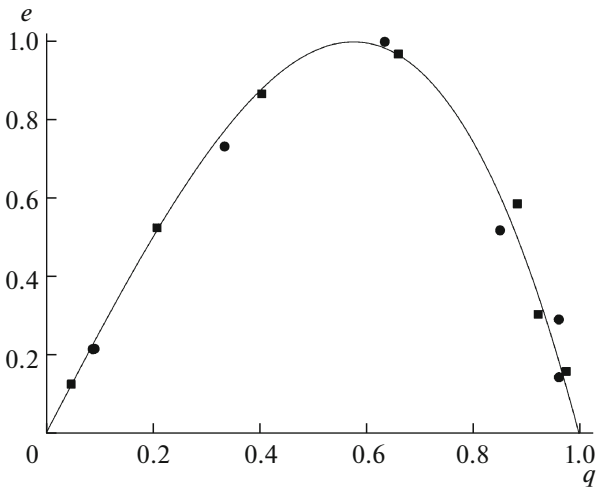

Fig. 9. Calculated dependences of relative efficiency e = $\mathrm{eff}/\mathrm{eff}_\mathrm{m}$ of apparatus on relative volume flow rate q of gas through apparatus for both diameters D_APP: (■) 140 and (●) 160 mm. Curve describes dependence $e = 3^{3/2}/2q(1-q^2)$.

CONCLUSIONS

In this study, the model of the spray produced by a nozzle, which was proposed earlier in [4, 9], has been developed. A comparison of the results of calculations of the two-phase flow based on this model with the experimental data leads to the conclusion that the numerical model described here makes it possible to analyze the turbulent two-phase flow with an admissible degree of accuracy.

The distinguishing features and advantages of this model are that it is applicable to a compressible continuous dispersion medium, as well as for an almost incompressible flow; it can be used to calculate nonstationary flows, as well as (quasi-)stationary states. The latter are obtained from the former states as a result of evolution. The difference equations of the given model make it possible to calculate all variables using a simple explicit scheme.

As compared to earlier publications of the author [4, 9], new results have been obtained in this study. In particular, the free spray with a height of up to 1 m was calculated in one run and not only in several runs on sequential regions of a smaller height. The results of new calculations for the velocities of the phases are in good agreement with experiment.

In addition to the free spray, we have calculated the two-phase gas–droplets flow in a cylindrical spraying apparatus. The dependences of maximal values of gas volume flow rate Q_m and pressure drop P_m in the apparatus on its diameter have been established, and the form of the dependences of hydraulic characteristic $P(Q)$ of the apparatus and its hydraulic efficiency $\mathrm{eff}(Q)$ on gas flow rate Q in the apparatus have been calculated. It has been shown that the peak of the hydraulic efficiency is attained under condition (22).

Taking into account the analogy between interfacial transfer of momentum, mass, and heat in a turbulent two-phase flow [13, 14], we can propose that the maximal efficiency of the heat and mass transfer in the spraying apparatus is attained under the same condition (22).

REFERENCES

1. R. I. Nigmatulin, *Dynamics of Many-Phase Systems* (Nauka, Moscow, 1987), Part 1.
2. G. N. Abramovich, *Theory of Turbulent Jets* (Nauka, Moscow, 1984).
3. N. N. Simakov, Tech. Phys. **49**, 188 (2004).
4. N. N. Simakov and A. N. Simakov, J. Appl. Phys. **97**, 114901 (2005).
5. L. B. Torobin and W. H. Gauvin, Can. J. Chem. Eng. **37** (4), 129 (1959).
6. H. Schlichting, *Boundary Layer Theory* (McGraw-Hill, 1960).
7. N. N. Simakov, Tech. Phys. **55**, 913 (2010).
8. N. N. Simakov, Tech. Phys. **58**, 481 (2013).
9. N. N. Simakov, Izv. Vyssh. Uchebn. Zaved., Khim. Khim. Tekhnol. **45** (7), 125 (2002).
10. L. G. Loitsyanskii, *Fluid and Gas Mechanics* (Nauka, Moscow, 1978).
11. D. E. Potter, *Computational Physics* (Wiley, London, 1973).
12. N. N. Simakov, Extended Abstract of Doctoral Dissertation in Mathematics and Physics (Yaroslavl State Technical Univ., Yaroslavl, 2003).
13. N. N. Simakov, Tech. Phys. **61**, 1312 (2016).
14. N. N. Simakov, Tech. Phys. **61**, 1806 (2016).

Translated by N. Wadhwa